TEMPERATURE-INSENSITIVE 2D RESONANT GAP-BASED STRAIN SENSOR

Xintian Liu, and Clark T.-C. Nguyen
University of California, Berkeley, California, USA

ABSTRACT

A micromechanical resonant strain sensor employing gap-dependent electrical stiffness across quad-emplaced electrodes enables precise two-dimensional (2D) strain measurement while achieving an *xy* cross-axis sensitivity less than 1.5% and remarkably small temperature sensitivities of 0.49με/ºC and 0.62με/ºC along the *x* and *y* axes, respectively, over a 20-80ºC range. This represents more than 5× improvement in cross-axis insensitivity and more than 83× enhancement in temperature stability vs a close-by polysilicon piezoresistive strain sensor on the same chip. Such low temperature dependence across two dimensions results from the use of electrical stiffness curve-fitting to extract differential electrode-to-resonator gaps, which negates Young's modulus temperature dependence.

KEYWORDS

ring resonator, strain gauge, quality factor, electrical stiffness

INTRODUCTION

Anisotropy of materials used in harsh environment applications, e.g., on an automobile, fuels a need for multi-dimensional strain sensing with low cross-axis sensitivity and temperature dependence. Indeed, 2D strain sensors can provide a more comprehensive strain topography map that better conveys early warning signs to prevent failure of critical parts, e.g., a hydrogen tank for a fuel cell car. Here, conventional metal foil strain gauges typically exhibit sizable temperature sensitivity of ~50με/ºC and suffer from lateral strain when sensing strain along one axis. A surface acoustic wave (SAW) strain sensors exhibits 4% cross-axis sensitivity after compensation from 24% [1]. While MEMS capacitive strain gauges [2] are fairly temperature insensitive, their cross-axis sensitivity can be on the order of 10%. Meanwhile, a resonant strain sensor employing electrode-to-resonator gap-based strain sensing recently permitted isotropic strain sensing with a temperature sensitivity of only 0.1με/ºC [3].

This work takes the gap-based resonant strain sensor concept to two dimensions and in so doing not only harnesses a similar low temperature dependence but also achieves strain sensing with a measured 26 nε resolution (4.5 nε theoretical) and an *xy* cross-axis sensitivity below 1.5%.

RING RESONATOR STRAIN GAUGE

Figure 1 presents a schematic view of the 2D gap-based resonant strain sensor, which like the device of [3], employs a spoke-supported polysilicon ring resonator surrounded by electrodes, but here spaced 70 nm from the ring edges. Unlike the isotropic strain sensing device of [3] which had a single-piece, unsegmented outer electrode and inner electrodes all electrically connected, the device of Figure 1 divides the inner and outer electrodes into four electrode pairs, each aligned to two orthogonal axes along which they can independently sense strain applied into the silicon substrate.

Here, strain introduced to the substrate induces a shift in the electrode-to-resonator gap spacing that serves as the main strain indicator. Figure 2 shows the cross-sectional view of the ring resonator: (a) in an unstressed state, with equal inner and outer gaps along x and y axes, and (b) after application of pure *x*-axis strain and no *y*-axis strain, resulting in a difference between the inner and outer gaps along the *x*-axis while gaps along the *y*-axis remain relatively unchanged. The *x*-axis strain is then $\varepsilon_x = (d_{out,x} - d_{in,x})/(2R)$ where Figure 1 defines the variables. Clearly, the strain sensing precision depends upon the precision to which the gap spacing can be measured. Here,

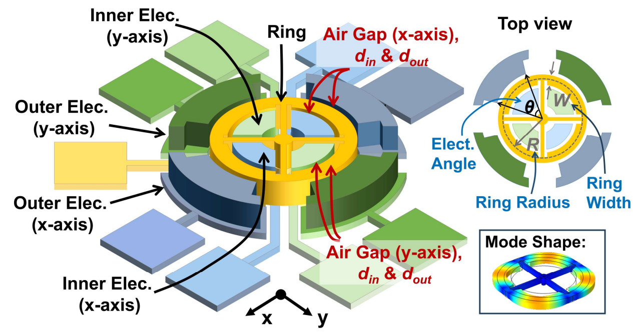

Figure 1: Perspective view of a ring resonator featuring isolated inner and outer electrodes along the x- and y-axes.

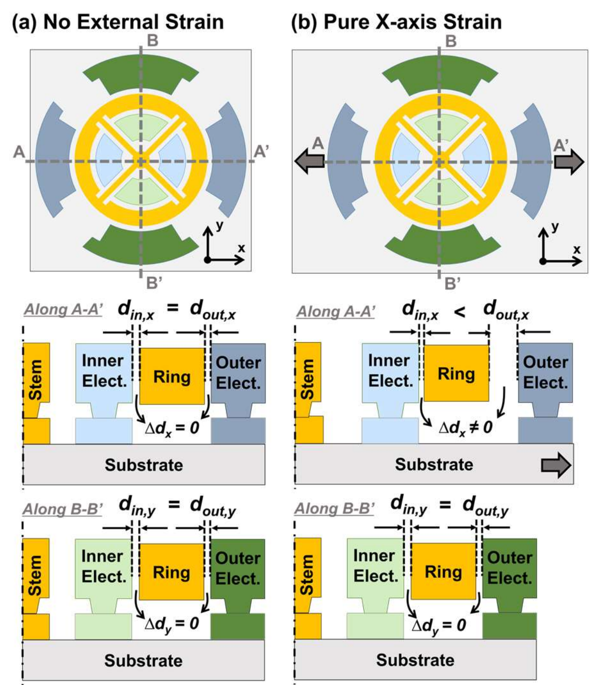

Figure 2 : Top and cross-sectional ring resonator views with (a) no external strain and (b) pure x-axis strain along A-A' and B-B'.

the electrical stiffness formed across each gap [4] provides a very precise method to extract the gap by curve-fitting of resonance frequency vs dc-bias voltage curves—a method that removes Young's modulus temperature dependence.

EXPERIMENTAL RESULTS

Figure 3 presents the SEM image of a fabricated gap-based strain sensing ring resonator (*cf.* Table 1) using the tiny-gap polysilicon surface micromachining process of [5]. For baseline comparison, the fabrication process also included polysilicon piezoresistive strain sensors oriented to detect strain in the *x* and *y* directions.

Figure 4(a) presents the measured frequency response of a fabricated ring resonator at room temperature taken from the ring electrode and outer *y*-axis electrode under 8mTorr vacuum provided by a Lakeshore FWPX probe station. The measured resonance

978-1-940470-05-4/HH2024/$25©2024TRF
DOI 10.31438/TRF.HH2024.123

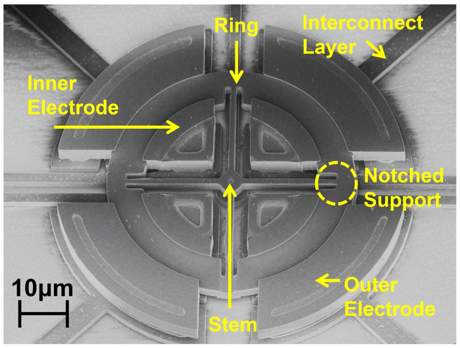

Figure 3: SEM image of a fabricated strain sensor.

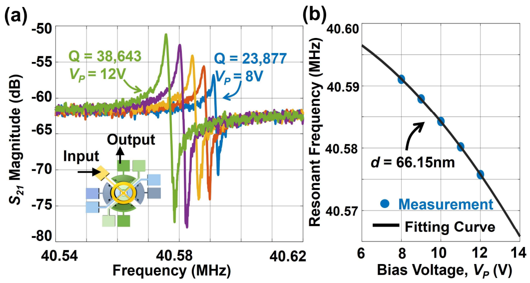

Figure 4: (a) Measured frequency spectra of the fabricated ring resonator with varying bias voltages from 8V to 12V. (b) gap spacing extraction from a resonance frequency versus bias voltage curve via curve-fitting.

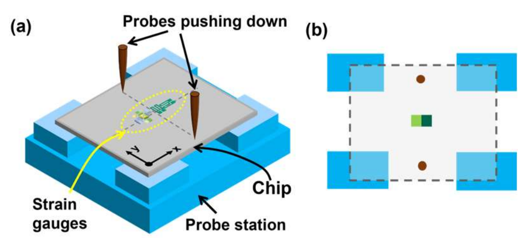

Figure 5: (a) Experimental apparatus employing probe station probes to apply x-axis strain to a chip housing strain gauges and (b) top view of uniaxial strain application along the x-axis.

Table 1: Polysilicon Gap-Based Resonant Strain Sensor Design

Parameter	Value	Parameter	Value
Ring Radius, R	18.75μm	Ring Width, W	6.5μm
Thickness, H	2μm	Gap, d_{in}/d_{out}	60nm
Elect. Angle, θ	60.2°	Res. Freq., f	45MHz

frequency and quality factor Q at 12V dc-bias voltage are 40.58 MHz and 38,643, respectively. Figure 4(b) illustrates extraction of the outer-electrode-to-ring gap along the y-axis by curve-fitting of frequency vs dc-bias, indicating a 66.145 nm gap.

To apply uniaxial (as opposed to isotropic) strain to the substrate housing the sensor, two probes press on the edges of the substrate die at the midpoint of the axis to be strained while the die sits atop a valley in the chuck, supported by mesas under its four corners, as shown in Figure 5, which illustrates the application of x-directed strain. The probes contact the die approximately 2 mm away from the sensor's central point.

Figure 6 compares bar charts summarizing the measured strain of a gap-based resonant strain gauge vs a close-by piezoresistive strain gauge when the probes apply only x-axis strain (left) and only y-axis strain (right). In response to x-axis strain, the gap-based

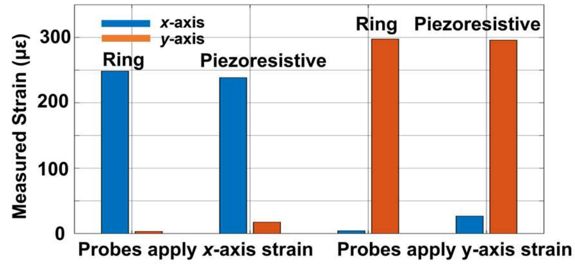

Figure 6: Measured strain of the gap-based resonant strain gauge compared with a close-by piezoresistive strain gauge.

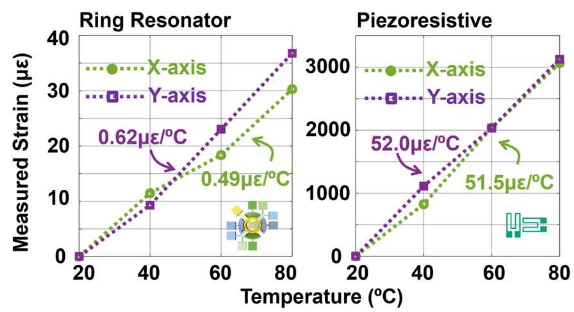

Figure 7: Measured strain vs temperature of the gap-based and piezoresistive strain gauge without externally applied strain.

resonant strain sensor reads 248.5με and 3.3με for the x-axis and y-axis, respectively, yielding a 1.32% cross-axis sensitivity, which is 5.5× better than that the 7.30% of the piezoresistive one. Under only y-axis strain, the gap-based strain sensor outputs 4.3με on the x-axis and 297.6με on the y-axis, for a 1.46% cross-axis sensitivity and a 6.2× improvement over the 9.03% of the piezoresistive device.

Finally, Figure 7 directly compares the temperature sensitivities of the gap-based and piezoelectric strain sensors. Here, the ring resonator exhibits 0.49με/°C x-axis and 0.62με/°C y-axis temperature coefficients over a 20°C to 80°C range, which are at least 83× better than the 51.50με/°C and 52.0με/°C, respectively, of the piezoresistive strain gauge.

CONCLUSION

By extending the applicability of a gap-based resonant strain sensing to 2D while retaining its inherent temperature insensitivity and exhibiting very low cross-axis sensitivity, the device demonstrated herein sets the stage for distributed precision strain sensing on complex surface geometries. Here, ensembles of tiny sensors sprinkled over a surface might provide a topographical strain map capable of pinpointing high-strain trouble spots that warn of imminent failure. The next step towards such a goal will likely entail integration with electronics that automate the described gap extraction process while providing a tiny chip-scale form factor.

REFERENCES

[1] R. Stoney, *et al.*, "Characterization of differentially measured strain using passive ...," DOI: 10.1109/JSEN.2013.2285722.
[2] B. Jamshidi, *et al.*, "Enhanced cross-axis rejection capacitive strain gauge," DOI: 10.1115/IMECE2007-43168.
[3] X. Liu, *et al.*, "Temperature-insensitive resonant strain sensor," DOI: 10.1109/EFTF/IFCS54560.2022.9850437.
[4] A. Ozguluk, *et al.*, "On-chip precision residual strain…," DOI: 10.1109/TRANSDUCERS.2019.8808299.
[5] M. Akgul, *et al.*, "RF channel-select micromechanical disk—Part II," DOI: 10.1109/TUFFC.2018.2883296.